JSR Publications

Available Online

J. Sci. Res. **17** (2), 417-425 (2025)

JOURNAL OF SCIENTIFIC RESEARCH

www.banglajol.info/index.php/JSR

Characterization of a Fluorinated Ferroelectric Liquid Crystal by Molecular Optimization Electro-Optic Study and SAXS

Debarghya Goswami*

Department of Physics, St. Joseph's College, Darjeeling 734104, India

Received 15 August 2024, accepted in final revised form 16 February 2025

Abstract

In this work a fluorinated ferroelectric liquid crystal has been characterized by molecular optimization, electro-optic study and small angle x-ray scattering (SAXS) to investigate its applicability for display and NLO applications and also to inculcate the relation between its structural conformation and bulk property. The optimized molecular structure of the compound was simulated and different molecular properties were calculated by means of quantum calculations (Hartree-Fock method). The phase behavior of the compound was studied by Polarized optical microscopy (POM) study. The Polarizing optical microscopy revealed a broad spectrum of ferroelectric SmC* phase and a short range SmA* phase in the compound. The electrical response time was measured and was found to be in micro second range. The layer spacing and the tilt angles of the molecules in SmC* phase was measured using SAXS. For its large thermal span of ferroelectric SmC* phase and response time in microsecond range the compound found to be potentially useful for formulating one ferroelectric room temperature liquid crystal mixture, appropriate for display applications.

Keywords: Ferroelctric liquid crystal; Polarizing optical microscopy; Response time; Hartree-Fock formalism.

doi: https://dx.doi.org/10.3329/jsr.v17i2.75460 J. Sci. Res. **17** (2), 417-425 (2025)

1. Introduction

Liquid crystal blends the distinctive properties of both solids and liquids as it combines the fluidity of liquid along with anisotropy of conventional solids. As a result, liquid crystals show exclusive electro-optical properties which has been proved to be useful for various applications, particularly in display technology. Although conventionally most liquid crystal displays (LCDs) available commercially utilize nematic liquid crystals, their slow response time makes them unfit for high-speed display applications. Whereas chiral liquid crystals having ferroelectric or antiferroelectric mesophases exhibit much sharper response time, making them suitable for fast display applications [1–4]. Thus, chiral liquid crystals are of current interest for display technology. Nevertheless, to use ferroelctric liquid crystals

* *Corresponding author*: sangdin@gmail.com

(FLCs) in display or other types of applications commercially, one need to tailor their electro-optic and phase properties in accordance to the need of the applications. Hence, it is important to know how the mesogenic properties of such compounds are interlinked with their molecular structure and molecular properties. This knowledge may help to synthesis new FLC compounds with desired properties suitable for specific application. For example, it has been reported by various research groups that liquid crystals with fluro-substitute typically display reduced viscosity, excellent thermal stability, minimal optical anisotropy attributed to the minute dimensions of a fluoro-substituent and strong C-F bonding [5–7]. Keeping that in mind one chiral ferroelectric liquid crystal viz. (S)-(+)-4′-[(3-pentadecafluorooctanoyloxy)prop-1-oxy]biphenyl-4-yl 4-(1-methylheptyloxy) benzoate (7F3R) has been selected for investigation [8,9]. Fig. 1 shows the molecular structure of 7F3R.

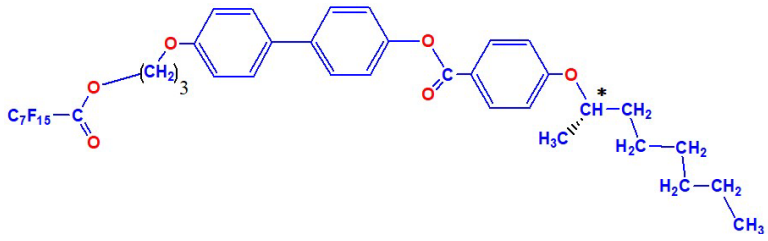

Fig. 1. Molecular structure of 7F3R.

The molecular geometry of the compound was optimized by Hartree-Fock method to inculcate the molecular properties of the compound. The optimized molecular length, dipole moment and the difference between the energy levels of Frontier Molecular Orbits were calculated. Compound's phase progression and corresponding transition temperatures which were already published [9] were reconfirmed using polarizing optical microscopy. The electrical response time which is one of the key parameters to explore applicability of FLCs in display devices was measured. The layer spacing and tilt angle in SmC* phase was measured using small angle X-ray scattering (SAXS) method.

2. Experimental Methods

To observe the textures of the compound the FLC sample was fed into a commercial dielectric cell of 5μm thickness. The optical textures were recorded by placing the cells in-between the crossed polarizer of Olympus BX41 polarizing microscope with magnification 10x and 20x which was furnished with a 5MP CCD camera. Same cell was employed to determine the electrical response time of the compound. Using reversal current method, the response time of the compound was measured by applying an ac square pulse (0.1-50V and 10-60 Hz) as the input wavefront through an Agilent 33220A function generator. The signal was amplified with the help of a FLC Electronics (Sweden) amplifier. Tektronix TDS 2012B digital oscilloscope was employed to record the voltage drop across a 100kΩ

resistance R in series with the sample cell, over time. Finally, to calculate the response time I measured the delay in time between the applied square pulse edge and the polarization bump as I track the voltage across the resistor R. The temperature (accuracy ±0.1 °C) was controlled utilizing a Mettler FP90 temperature controller with FP84HT hot stage.

To perform SAXS, the sample was fade into a capillary in random orientation. Ni filtered CuKα radiation was used as the source. Photographs were recorded in photographic plates inside a specially designed camera capable of enduring high temperature. Layer spacing and tilt angles of the compound was calculated by analyzing the photographs. The detail procedures of this experiment were described in earlier publications [10].

3. Results and Discussion

3.1. *Optimized molecular geometry*

The overall characteristics of the FLCs are greatly influenced by their molecular structure and its conformity. To explore its molecular configuration the 3D molecular structure of the compound was optimized by Hartree-Fock method with 3-21G basis set using a software tool [11]. The optimized molecular length along with the dipole moment of 7F3R were previously reported using PM3 method [9]. Compared to other quantum calculation methods PM3 is numerically much less intensive and thus less time consuming. However, PM3 uses semi empirical approach to estimate an approximation of Hartree-Fock (HF) method. In contrast Hartree-Fock is much more comprehensive. It is an ab initio method. In HF method the time independent Schrodinger equation of the many body systems (the electron distribution of molecule in this case) is solved to explore the electronic configuration and energy of the system. In this method the effect of Pauli's exclusion principle is incorporated by including a Slater determinant in the wave function. HF method initiates with a preliminary estimation of electron distribution and continuously adjust the initial value through repetitive iterations to ultimately reach in a self-consistent value and finally the energy and distribution of the electron of the system is calculated. Thus Hartree-Fock method is a much more reliable compared to PM3 method [12]. The optimized structure as well as direction of dipole moment is shown in Fig. 2.

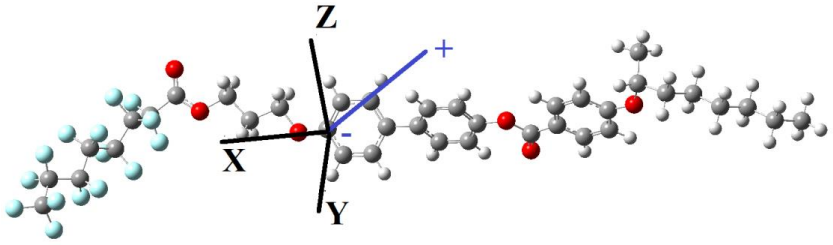

Fig. 2. Optimized geometry of 7F3R.

The optimized length (*l*) of 7F3R was determined to be 37.01Å. As expected, it was found to be longer than another compound of the same homologous series 5F3R [13] . The

optimized value of dipole moment (μ) of 7F3R was 6.55 D (-5.06, 0.4784, 4.14) (the components of μ along x, y and z axes respectively mentioned in bracket). The dipole moment is also found to be marginally larger than 5F3R which is also expected due to the existence of the additional fluorine atoms in this compound.

The applicability of FLCs for Nonlinear applications (NLO) and its photochemical stability can be assessed from the difference of energy (∇ε) between the highest occupied molecular orbit (HOMO) and lowest unoccupied molecular orbit (LUMO) of Frontier Molecular Orbit's (FMO's). The value of ∇ε also helps to estimate the capability of the molecule to move electron from HOMO to LUMO orbital at the time of electronic excitation process [12,14,15] . The HOMO and LUMO surfaces of 7F3R have been simulated by the same optimization method and the orbits are shown in Fig. 3. It is clear from Fig. 3 that the HOMO and LUMO have a high degree of delocalization.

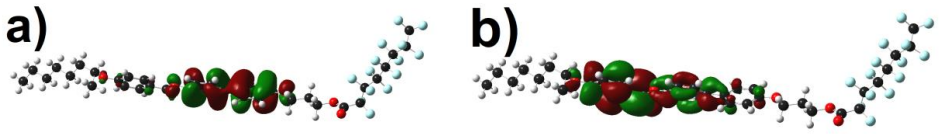

Fig. 3. The a) HOMO and b) LUMO of 7F3R.

HOMO can be seen around the biphenyl part of the core, while the LUMO is stretched throughout the core including the third phenyl ring. Similar positions of HOMO and LUMO was reported for another compound of same homologous series [13]. The band gap (∇ε) of the compound was calculated to be -0.39 au. The value of ∇ε was small which indicates that 7F3R can be easily polarizable. Some reactivity parameters of 7F3R have been calculated using FMO data and standard equations [16]which have been listed on Table 1.

Table 1. Reactivity parameters of 7F3R (all parameters are quoted in au).

Electron affinity (A)	Ionization potential (I)	Electronegativity (χ)	Global hardness (η)	Global softness (μ)	Global electrophilicity index (ω)
-0.095	0.29876	0.102	-0.39	-2.56	8.4

From the value of HOMO LUMO gap and the reactivity parameters it can be concluded that the compound may be suitable for NLO applications for example telecommunication, signal processing, optical interconnection etc.

3.2. *Polarized optical microscopy (POM) study*

POM is a useful tool to inculcate the phase sequence as well as phase transition temperatures of any liquid crystal compound. Liquid crystals are optically anisotropic in nature. Due to its birefringent property liquid crystal compounds show optical textures when illuminated in between a cross polarizer. On top of it due to diverse structures and different topological defects of different phases, they can be distinguished by their typical optical textures. For

example, in SmA* phase, the smectic layers are arranged in Dupin cyclides with a pair of focal conics, due to which the most commonly observed optical texture in SmA* phase is that of a fan shaped texture. On the other hand, the SmC* phase which results from cooling SmA* phase is typically identified by broken fan-shaped texture. Only difference in the structure of SmA* and SmC* phase is that in SmA* phase the molecular director aligns itself in the direction of the layer normal, in SmC* it is tilted. As in SmC* phase the tilt is random to some extent, tiny regions of different tilt appear at the boundaries of fan shape texture. This is how the broken fan-shaped originates [17].

The optical texture of 7F3R was determined in homogeneous geometry in cooling cycle. The textures of 7F3R in different phases are depicted in Fig. 4. After isotropic phase a signature fan shaped texture was observed from 151.1 °C to 148 °C which confirmed that 7F3R exhibits SmA* phase in this temperature range. In the range of 148 °C to 75.5 °C, the broken fan shape texture was noticed, accompanied by slight alternation in birefringence which signifies SmC* phase in this range of temperature. Usually for chiral compounds it can be possible to see parallel chiral lines superimposed on the texture of SmC* phase. However, chiral lines were not observed in SmC* texture of 7F3R. Sometimes, the lack of chiral lines is linked to the reduced pitch length of the compounds [17,18]. It can be mentioned here that for LC compounds of other series, for the compounds with high number of fluorine atoms the pitch was reported to be short [8]. Below 75.5 °C the compound showed optical texture of crystalline solids. The compound's phase sequence has been summarized in Table 2. The phase sequence observed by POM matches exactly with the phase sequence reported before by other experimental methods [8,9]. It can be noted that the compound exhibits SmC* phase for large span of temperature (72.5 °C). This makes the compound promising to be used as a dopant to formulate FLC mixture suitable for display applications.

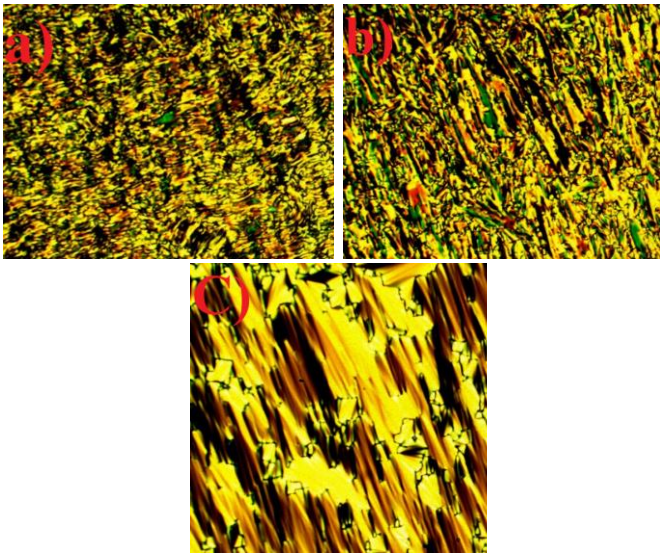

Fig. 4. Optical texture of 7F3R at a) SmA* (149 °C) b) SmC* (114 °C) and c) Crystal (74 °C).

Table 2. Phase sequence of 7F3R.

Compound	Phase sequence	Stability of SmC* phase
7F3R	Crystal: 75.5 °C: SmC*148.0 °C: SmA*: 151.1 °C: Isotropic	72.5 °C

3.3. *Electrical response time (τ)*

Response time is a crucial factor of ferroelectric liquid crystals from application viewpoint. It indicates how quickly the molecules can response to some external electric field in that phase. FLCs with smaller response time are ideal for high-speed display uses. Usually in ferroelectric SmC* phase LCs exhibit μs range response to electric field which is much faster than its nematic counterpart (ms range) [19,20]. The temperature variation of the response time of 7F3R in SmC* phase is shown in Fig. 5.

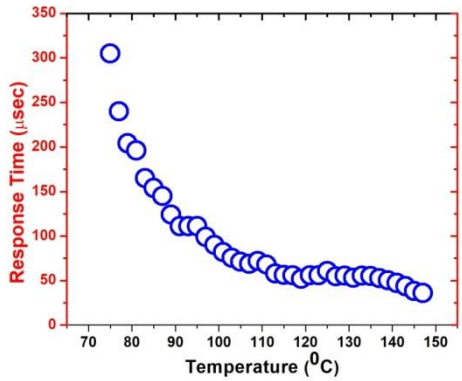

Fig. 5. Temperature variation of response time of 7F3R.

The response time was found to be maximum (300 μs) at lowest temperature of SmC* phase and then decreased rapidly. It became minimum near SmC*-SmA* (below 50 μs). Compounds having high dipole moment usually interact quickly with external electric field and show smaller electric response time. Thus, the high value of the optimized dipole moment of 7F3R is in conformity with its sharp response time. This small value of electric response time implies once again that 7F3R can potentially be used as a dopant to design a room temperature FLC mixture suitable for fast display applications.

3.4. *SAXS measurements*

The layer spacing (d) of the SmC* phase was calculated from the diffused inner ring of the X-ray diffraction photograph of the randomly oriented sample. The temperature variations of the layer spacing, determined by studying the diffraction photographs, are illustrated in Fig. 6a. Layer spacing in SmC* phase was found to be less than the optimized length which is anticipated due to the inherent tilt of the molecules with respect to the layer normal in this phase. A nonlinear increasing trend of the layer spacing was observed in SmC* phase

as temperature rose. It increased from 27.7 Å-33 Å. This happened as the molecular tilt angle in SmC* phase reduces with increasing temperature under the rigid rod approximation of molecular structure. This type of temperature variation of layer spacing have been reported before for other compounds in same homologous series [10].

The molecular tilt angle (θ) in SmC* phase, which is also the primary order parameter of the phase, was determined employing the formula $\theta = \cos^{-1}(d/l)$, l being the optimized molecular length. The tilt angle at smaller temperature was found to be quite high (~47°) and gradually decreased with temperature. The dependence of tilt angle with temperature is in conformity with the generalised mean field theory for SmC* to SmA* phase transition [21]. Fig. 6b illustrates the change in tilt angle with temperature for the selected compound. It is worth mentioning that FLC compounds with huge tilt angles as 7F3R are ideal materials to design micro-optic switch for multimode fibre which are based on total internal reflection. Furthermore, under suitable surface anchoring, these type of high tilt materials can also be useful in designing display devices capable of rendering gray scale [22].

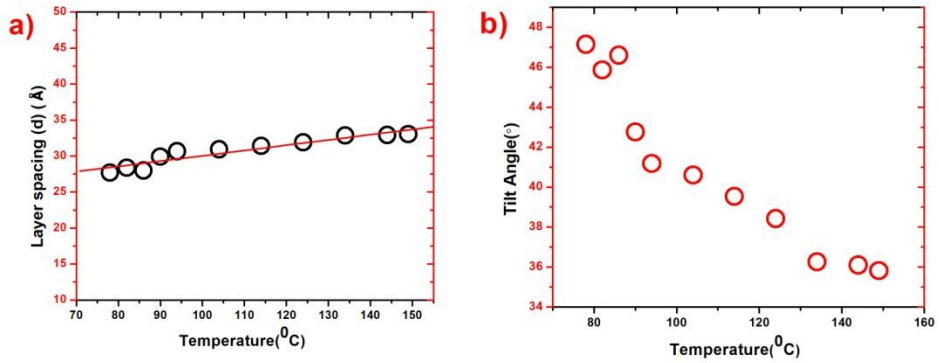

Fig. 6. Temperature variation of a) layer spacing and b) tilt angle of 7F3R in SmC* phase.

4. Conclusion

The Hartree-Fock method with 3-21G basis had been employed to optimize the molecular geometry of the selected ferroelectric liquid crystal compound 7F3R. The compound exhibits a high dipole moment as expected for fluorinated ferroelectric liquid crystals and also a long molecular length. The positions of the HOMO and LUMO were estimated and band gap was calculated. The large band gap between HOMO and LUMO implied that the compound has high photochemical stability. From the values of reactivity parameters, calculated from FMO data, the compound was found to be promising for NLO applications. Polarizing optical microscopy was employed to confirm the compound's phase sequence as well as transition temperatures. It was found to have a long-range ferroelectric SmC* phase and a short range SmA* phase. The electrical response time was found to be quite sharp in micro second range. The SAXS study revealed moderate value of layer spacing in SmC* phase which increased with temperature. This temperature variation of the layer spacing

was attributed with the decrease of SmC* tilt angle. To confirm this tilt was measured with a rigid molecule approximation. The X-ray tilt at smaller temperature was found to be quite large (~47°) and it decreased with temperature as expected. This kind of high tilt angle may be appropriate for display devices with grayscale capabilities as well as micro-optic switches for multimode fiber that rely on total internal reflection. Though the compound can't be directly used for display applications as the temperature range of its ferroelectric liquid crystal phase is way above room temperature but for its wide temperature range of SmC* phase and μs range electrical response time it can potentially be used as a dopant to design room temperature ferroelectric liquid crystal mixture suitable for fast display applications.

Acknowledgment

The author is grateful to R. Dabrowski, Military institute of technology, Warsaw, Poland for kindly supplying the liquid crystal sample. The author also likes to thank P. K. Mandal, Department of Physics, University of North Bengal, for kindly allowing the author to use his laboratory.

References

1. D. Demus, J. Goodby, and G. W. Gray, Handbook of Liquid Crystals (WILEY-VCH, New York, 1998). https://doi.org/10.1002/9783527620593
2. I. Muševic, R. Blinc, and B. Zekš, The Physics of Ferroelectric and Antiferroelectric Liquid Crystals, The Physics of Ferroelectric and Antiferroelectric Liquid Crystals (World Scientific, Singapore, 2000). https://doi.org/10.1142/1173
3. R. B. Meyer, L. Liebert, and L. S. et P. Keller, J. Phys. Lett. **36,** 69 (1975). https://doi.org/10.1051/jphyslet:0197500360306900
4. A. Debnath and P. K. Mandal, J. Mol. Liq. **221**, 287 (2016). https://doi.org/10.1016/j.molliq.2016.06.001
5. P. Morawiak, W. Piecek, M. Żurowska, P. Perpowskin, Z. Raszewski, et al., Opto-Electronics Rev. **17**, 40 (2009). https://doi.org/10.2478/s11772-008-0044-x
6. C. Yang, F. Ye, X. Huang, J. Li, X. Zhang et al., Liq. Cryst. **51**, 558 (2024). https://doi.org/10.1080/02678292.2024.2306309
7. T. K. Abhilash, H. Varghese, M. Czerwiński, K. Czupryński, and A. Chandran, J. Mol. Liq. **341**, ID 117392 (2021). https://doi.org/10.1016/j.molliq.2021.117392
8. D. Ziobro, R. Dąbrowski, M. Tykarska, W. Drzewiński, M. Filipowicz et al., Liq. Cryst. **39**, 1011 (2012). https://doi.org/10.1080/02678292.2012.691560
9. D. Goswami, A. Debnath, P. K. Mandal, D. Weglowska, R. Dabrowski et al., Liq. Cryst. **43,** 1548 (2016). https://doi.org/10.1080/02678292.2016.1186755
10. D. Goswami, D. Sinha, A. Debnath, S. K. Gupta, W. Haase et al., J. Mol. Liq. **182**, 95 (2013). https://doi.org/10.1016/j.molliq.2013.03.002
11. Gaussian 98, Revision A.11.4, M. J. Frisch, G. W. Trucks, H. B. Schlegel, G. E. Scuseria, M. A. Robb et al., (Gaussian, Inc., Pittsburgh PA, 2002).
12. D. Sharma and S. N. Tiwari, Emerging Mater. Res. **6**, 322 (2017). https://doi.org/10.1680/jemmr.15.00052

13. D. Goswami, J. Sci. Res. **16**, 97 (2024). https://doi.org/10.3329/jsr.v16i1.65364
14. D. Goswami, Mol. Cryst. Liq. Cryst. **767**, 86 (2023). https://doi.org/10.1080/15421406.2023.2228642
15. N. H. S. Ahmed, G. R. Saad, H. A. Ahmed, and M. Hagar, RSC Adv. **10**, 9643 (2020). https://doi.org/10.1039/C9RA10499B
16. R. K. Sah and A. Bhattacharjee, J. Mol. Struct. **1324**, ID 140832 (2025). https://doi.org/10.1016/j.molstruc.2024.140832
17. I. Dierking, Textures of Liquid Crystals (Wiley-VCH Verlag GmbH & Co. KGaA, New York, 2003). https://doi.org/10.1002/3527602054
18. D. Demus, Textures of Liquid Crystals (Verlag Chemie Weinheim, New York, 1978).
19. I. Dierking, Symmetry **6**, 444 (2014). https://doi.org/10.3390/sym6020444
20. P. Collings and J. Frankl. Inst. **342**, 599 (2005). https://doi.org/10.1016/j.jfranklin.2005.07.002
21. C. S. Hartley and N. Kapernaum, and J. C. Roberts, F. Giesselmann, R. P. Lemieux, et al., J. Mater. Chem. **16**, 2329 (2006). https://doi.org/10.1039/b515313a
22. E. P. Haridas, S. S. Bawa, A. M. Biradar, and S. Chandra, Jpn. J. Appl. Phys. **34**, 3602 (1995). https://doi.org/10.1143/JJAP.34.3602